Article

Elastic and Inelastic Electron Tunneling Spectroscopy of a New Rectifying Monolayer

Andrei Honciuc, Robert M. Metzger, Aijun Gong, and Charles W. Spangler

J. Am. Chem. Soc., **2007**, 129 (26), 8310-8319• DOI: 10.1021/ja068729g • Publication Date (Web): 07 June 2007

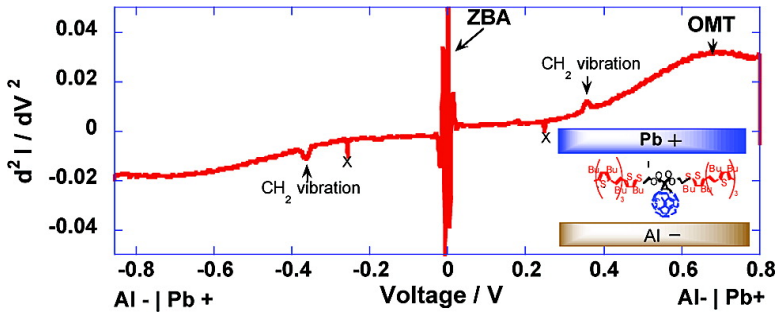

More About This Article

Additional resources and features associated with this article are available within the HTML version:

- Supporting Information
- Links to the 3 articles that cite this article, as of the time of this article download
- Access to high resolution figures
- Links to articles and content related to this article
- Copyright permission to reproduce figures and/or text from this article

View the Full Text HTML

J|A|C|S
ARTICLES
Published on Web 06/07/2007

Elastic and Inelastic Electron Tunneling Spectroscopy of a New Rectifying Monolayer

Andrei Honciuc,[†,‡] Robert M. Metzger,*[,†] Aijun Gong,[§,⊥] and Charles W. Spangler[§,||]

Contribution from the Laboratory for Molecular Electronics, Chemistry Department, University of Alabama, Tuscaloosa, Alabama 35487-0336, and Department of Chemistry, Montana State University, Bozeman, Montana 59717

Received December 5, 2006; E-mail: rmetzger@ua.edu

Abstract: Rectification of electrical current was observed in a Langmuir−Schaefer monolayer of fullerene-bis[ethylthio-tetrakis(3,4-dibutyl-2-thiophene-5-ethenyl)-5-bromo-3,4-dibutyl-2-thiophene] malonate, Au electrodes at room temperature (there are two regimes of asymmetry, at lower bias, i.e., between 0 and ±2 V, and at higher bias), and also between Pb and Al electrodes at 4.2 K. The latter experiment was coupled with second harmonic detection of the second derivative of the current with respect to voltage (d^2I/dV^2). The d^2I/dV^2 spectrum shows intramolecular vibrations, and also two antisymmetric broad bands, centered at ±0.65 V, due to resonant electron tunneling between the Fermi level(s) of the electrodes and the lowest unoccupied molecular orbital of the molecule.

Introduction

Electrical rectification in "metal|organic monolayer|metal" (MOM) junctions is a fundamental problem of asymmetric electron transfer across one "electroactive" molecule (or many molecules in parallel), but may also lead to single organic molecules as components for future nanoscopic organic electronic devices.

The first proposed mechanism for electrical rectification by a single molecule was that of Aviram and Ratner:[1] At different values of forward and reverse bias, the molecular energy levels of the donor and acceptor are brought differently into resonance with the Fermi level of the (macroscopic) metal electrodes, and the current−voltage plot ($I-V$ curve) should be asymmetric with respect to positive and negative bias.[2] Many unimolecular rectifiers have been studied;[3−11] single-molecule measurements by scanning tunneling microscopy have yielded several other rectifiers.[12−16] Most of these studies coupled the measured $I-V$ curves with a theoretical and ancillary spectroscopic characterization of these electroactive molecules, in solution, in bulk, and in monolayers. The purpose was to associate the highest occupied molecular orbital (HOMO), the lowest unoccupied molecular orbital (LUMO), and the electrode Fermi energies with the onset of enhanced electron current beyond a critical forward bias ("turn-on voltage"). The mechanism of electron transport in molecules and molecular wires is not completely elucidated. Spectroscopic studies of the monolayer under electrical bias are severely limited by the difficulty of probing the molecules within the MOM junction by sensitive spectroscopic methods.[17,18]

Theoretical calculations provide excellent insights[19−22] into the electrical conduction through a molecule by Landauer's

† University of Alabama.
‡ Present address: Department of Chemical and Biological Engineering, University of Colorado, Boulder, CO 80309-0424.
§ Montana State University.
⊥ Present address: Department of Chemistry, University of Rochester, Rochester, NY 14627.
|| Present address: Rastris, 2100 Fairway Dr., Suite 104, Bozeman, MO 58715.

(1) Aviram, A.; Ratner, M. *Chem. Phys. Lett.* **1974**, *29*, 277−283.
(2) Stokbro, K.; Taylor, J.; Brandbyge, M. *J. Am. Chem. Soc.* **2003**, *125*, 3674−3675.
(3) Metzger, R. M. *Chem. Phys.* **2006**, *326*, 176−187.
(4) Metzger, R. M.; Chen, B.; Höpfner, U.; Lakshmikantham, M. V.; Vuillaume, D.; Kawai, T.; Wu, X.; Tachibana, H.; Hughes, T. V.; Sakurai, H.; Baldwin, J. W.; Hosch, C.; Cava, M. P.; Brehmer, L.; Ashwell, G. J. *J. Am. Chem. Soc.* **1997**, *119*, 10455−10466.
(5) Metzger, R. M.; Xu, T.; Peterson, I. R. *J. Phys. Chem. B* **2001**, *105*, 7280−7290.
(6) Honciuc, A.; Otsuka, A.; Wang, Y.-H.; McElwee, S. K.; Woski, S. A.; Saito, G.; Metzger, R. M. *J. Phys. Chem. B* **2006**, *110*, 15085−15093.
(7) Baldwin, J. W.; Amaresh, R. R.; Peterson, I. R.; Shumate, W. J.; Cava, M. P.; Amiri, M. A.; Hamilton, R.; Ashwell, G. J.; Metzger, R. M. *J. Phys. Chem. B* **2002**, *106*, 12158−12164.
(8) Metzger, R. M.; Baldwin, J. W.; Shumate, W. J.; Peterson, I. R.; Mani, P.; Mankey, G. J.; Morris, T.; Szulczewski, G.; Bosi, S.; Prato, M.; Comito, A.; Rubin, Y. *J. Phys. Chem. B* **2003**, *107*, 1021−1027.
(9) Honciuc, A.; Jaiswal, A.; Gong, A.; Ashworth, K.; Spangler, C. W.; Peterson, I. R.; Dalton, L. R.; Metzger, R. M. *J. Phys. Chem. B* **2005**, *109*, 857−871.
(10) Shumate, W. J.; Mattern, D. L.; Jaiswal, A.; Dixon, D. A.; White, T. R.; Burgess, J.; Honciuc, A.; Metzger, R. M. *J. Phys. Chem. B* **2006**, *110*, 11146−11159.
(11) Oleynik, I. I.; Kozhushner, M. A.; Posvyanskii, V. S.; Yu, L. *Phys. Rev. Lett.* **2006**, *96*, 09803-1−09803-4.
(12) Ashwell, G. J.; Tyrrell, W. D.; Whittam, A. J. *J. Mater. Chem.* **2003**, *13*, 2855−2857.
(13) Ashwell, G. J.; Chwialkowska, A.; High, L. R. H. *J. Mater. Chem.* **2004**, *14*, 2848−2851.
(14) Ashwell, G. J.; Berry, M. *J. Mater. Chem.* **2005**, *15*, 108−110.
(15) Ashwell, G. J.; Tyrrell, W. D.; Whittam, A. J. *J. Am. Chem. Soc.* **2005**, *126*, 7102−7110.
(16) Morales, G. M.; Jiang, P.; Yuan, S.; Lee, Y.; Sanchez, A.; You, W.; Yu, L. *J. Am. Chem. Soc.* **2005**, *127*, 10456−10457.
(17) Nowak, A. M.; McCreery, R. L. *J. Am. Chem. Soc.* **2004**, *126*, 16621−16631.
(18) Jaiswal, A.; Tavakoli, C. G.; Zou, S. *Anal. Chem.* **2006**, *78*, 120−124.
(19) Krzeminski, C.; Delerue, C.; Allan, G.; Vuillaume, D.; Metzger, R. M. *Phys. Rev.* **2001**, *B64*, #085405.
(20) Gonzalez, C.; Manso-Simon, Y.; Batteas, J.; Marquez, M.; Ratner, M.; Mujica, V. *J. Phys. Chem. B* **2004**, *108*, 18414−18420.
(21) Mujica, V.; Ratner, M. A.; Nitzan, A. *Chem. Phys.* **2002**, *281*, 147−150.
(22) Mujica, V.; Nitzan, A.; Datta, S.; Ratner, M. A.; Kubiak, C. P. *J. Phys. Chem. B* **2003**, *107*, 91−95.

10.1021/ja068729g CCC: $37.00

theory,[23] using Green's functions for quantum transport phenomena and basis sets obtained by density-functional-theory or Hartree−Fock methods for the molecule and various approximate models for the electrode's density of states. This computes the coupling of the molecule with the electrodes and estimates the electron transport rates. However, charge trapping, monoradical ion formation, and even adiabatic electronic transitions in the molecule may also have to be considered.

One can assume that the total current passing through a MOM junction has three components: (1) the elastic (i.e., lossless) current due to tunneling through space, (2) the elastic current due to tunneling through molecular orbitals, and (3) the inelastic current due to electron scattering within the molecule.

Tunneling through space may be the largest contribution, especially when the Fermi energies are not in resonance with a relevant molecular orbital.[24]

Resonant tunneling current is expected to occur when the Fermi level of the electrode is in resonance with (i.e., has the same energy as) an unoccupied or partially occupied molecular orbital. This through-molecule current, also called orbital-mediated tunneling (OMT), can be a large part of the overall current.[25,26]

In general, inelastic processes involve electron transfer between metal and an organic or inorganic molecule O with the formation of a stable molecular anion O^- or cation O^+; this inelastic process is accompanied by a Franck−Condon rearrangement of the molecular geometry. Under these conditions, the molecular transition ($O \rightarrow O^+$ or $O \rightarrow O^-$) is termed adiabatic, and is generally slower. In contrast, an elastic process implies a resonant transfer, with no change in molecular geometry, and is associated with a vertical transition ($O \rightarrow O^+$ or $O \rightarrow O^-$) with no vibrational relaxation; such an elastic process is generally faster.[27]

Inelastic effects, due to vibronic excitation, generally bring a small contribution to the overall current, and occur at low biases.[28] In addition, electronic transitions within the molecule, vertical or adiabatic, excited by the tunneling electrons, can occur at higher voltages. These also bring a contribution to the overall current, as seen in some electron tunneling spectroscopy experiments.[26,29,30]

In this study, $I-V$ measurements show that a Langmuir−Schaefer (LS) monolayer of **1** (Figure 1A) exhibits current asymmetries, i.e., rectification, when sandwiched between two Au electrodes at room temperature. $I-V$ measurements and electron tunneling studies were carried out at 4.2 K on the same LS monolayer of **1**, now sandwiched between Al and Pb electrodes. Electron tunneling spectroscopy can probe molecular electronic states.[29,30] At low biases, molecular vibrations are expected and are observed as peaks in the second derivative of the current with respect to voltage (d^2I/dV^2). At higher applied voltages, molecular energy states were also observed and were more intense for forward than for reverse bias. This effect correlates well with the current asymmetries observed in the $I-V$ measurements. At much higher applied voltages, the rectification reverses direction. A thorough analysis of the monolayer orientation, vibration intensity changes for forward and reverse bias, and other studies relevant to the electron transport in MOM junction are also reported.

Experimental Details

The synthesis of **1** is documented in the Supporting Information (Figures A and B).

Ultraviolet−visible (UV−vis) spectra were acquired with a Cary 50 single-beam spectrometer, using a quartz cuvette of 1 cm path length. Fluorescence spectra were acquired with a Yvon-Jobin Fluoromax 2 spectrometer, using a quartz cuvette (1 cm path length) and a sample concentration of 2.5×10^{-6} mol/L.

Near-infrared and infrared spectra were acquired with a Bruker IFS-88 FTIR spectrometer, equipped with globar and tungsten sources and cryocooled detectors: mercury cadmium telluride (MCT) for the mid-infrared range and InSb for the near-infrared range. For each spectrum, a 1000-scan interferogram was collected in a single-beam mode with a 4 cm^{-1} resolution. The incident angle of the p-polarized light was set to 87° relative to the substrate normal.

Pockels−Langmuir (PL) monolayers at the air−water interface and LS and Langmuir−Blodgett (LB) transfers onto solid substrates were carried out with a NIMA 622 computer-controlled film balance in a room with HEPA-filtered air. The water subphase (18 MΩ cm) was obtained from a Barnstead Easypure LF system.

XPS spectra were obtained with a Physical Electronics Apex XPS system equipped with an Omicron EA125 hemispherical analyzer; the sample analysis chamber had a base pressure of 7×10^{-9} Torr, and Mg Kα (1253.6 eV) radiation was used as the excitation source. The scan parameters were set for a 25 eV pass energy and a 0.02 eV step scan; six scans were collected and averaged for each high-resolution spectrum.

The water contact angles of the LS films were determined with a Ramé-Hart contact-angle goniometer. The contact angle was read in one side of a drop on five different regions of the monolayer.

Variable-angle spectroscopic ellipsometry measurements were performed on a J. A. Woolam spectroscopic ellipsometer in the wavelength range 300−850 nm at 65°, 70°, and 75° angles of incidence.

The "Au|LS monolayer|Au" junctions used for electrical measurements were made by thermal evaporation of 5 nm Cr, then 115 nm Au onto a superpolished glass substrate (forming a film 120 nm thick), followed by LS monolayer deposition and evaporation of a second electrical contact by cold-gold technique[5] in an Edwards 306A evaporator (base pressure ≈ 10^{-7} Torr) equipped with a cold finger cooled externally with liquid N_2, and several temperature monitors and quartz film thickness monitors. During the deposition of the second electrical contact, on top of the organic monolayer, the substrates were placed on the cold finger, which was kept at a measured temperature of 150 K. The substrates were facing away from the evaporation source, to avoid organic monolayer decomposition due to radiation. Each glass slide would bear about 50 separate Au top "pads" 40 nm thick and 0.28 mm^2 in area. For the IETS measurements the "Al|LS monolayer|Pb" junctions were prepared similarly, except that the second electrical contact, Pb, was evaporated with the sample facing directly the evaporation source; during evaporation the substrate was also cooled to 170 K, to avoid the organic monolayer decomposition due to hot Pb atoms. During exposure of the Al substrates to moderate vacuum in the evaporator, and then to atmospheric air and water vapor, an oxide film of some thickness forms naturally atop the Al electrode. Each "Al|LS monolayer|Pb" junction has a working area of 0.5 mm × 2 mm. The Al thickness was ∼150 nm; the Pb thickness was ∼600 nm.

Conventional $I-V$ curves were measured with a Keithley 226 current−voltage source and monitor. The rectification ratio for any $I-V$ curve is defined by $RR = -I(V_{max})/I(-V_{max})$, where V_{max} is the maximum bias used to measure the $I-V$ curve.

(23) Landauer, R. *IBM J. Res. Dev.* **1957**, *1*, 223−231.
(24) Simmons, J. G. *J. Appl. Phys.* **1963**, *34*, 1793−1803.
(25) Mazur, U.; Hipps, K. W. *J. Phys. Chem.* **1995**, *99*, 6684−6688.
(26) Mazur, U.; Hipps, K. W. *J. Phys. Chem. B* **1999**, *103*, 9721−9727.
(27) Zhou, X.-L., Zhu, X.-Y.; White, J. M. *Surf. Sci. Rep.* **1991**, *13*, 73−220.
(28) Lambe, J.; Jaklevic, R. C. *Phys. Rev.* **1968**, *165*, 821−833.
(29) Hipps, K. W.; Mazur, U. *J. Am. Chem. Soc.* **1987**, *109*, 3861−3865.
(30) Lüth, H.; Roll, U.; Ewert, S. *Phys. Rev. B* **1978**, *18*, 4241−4249.

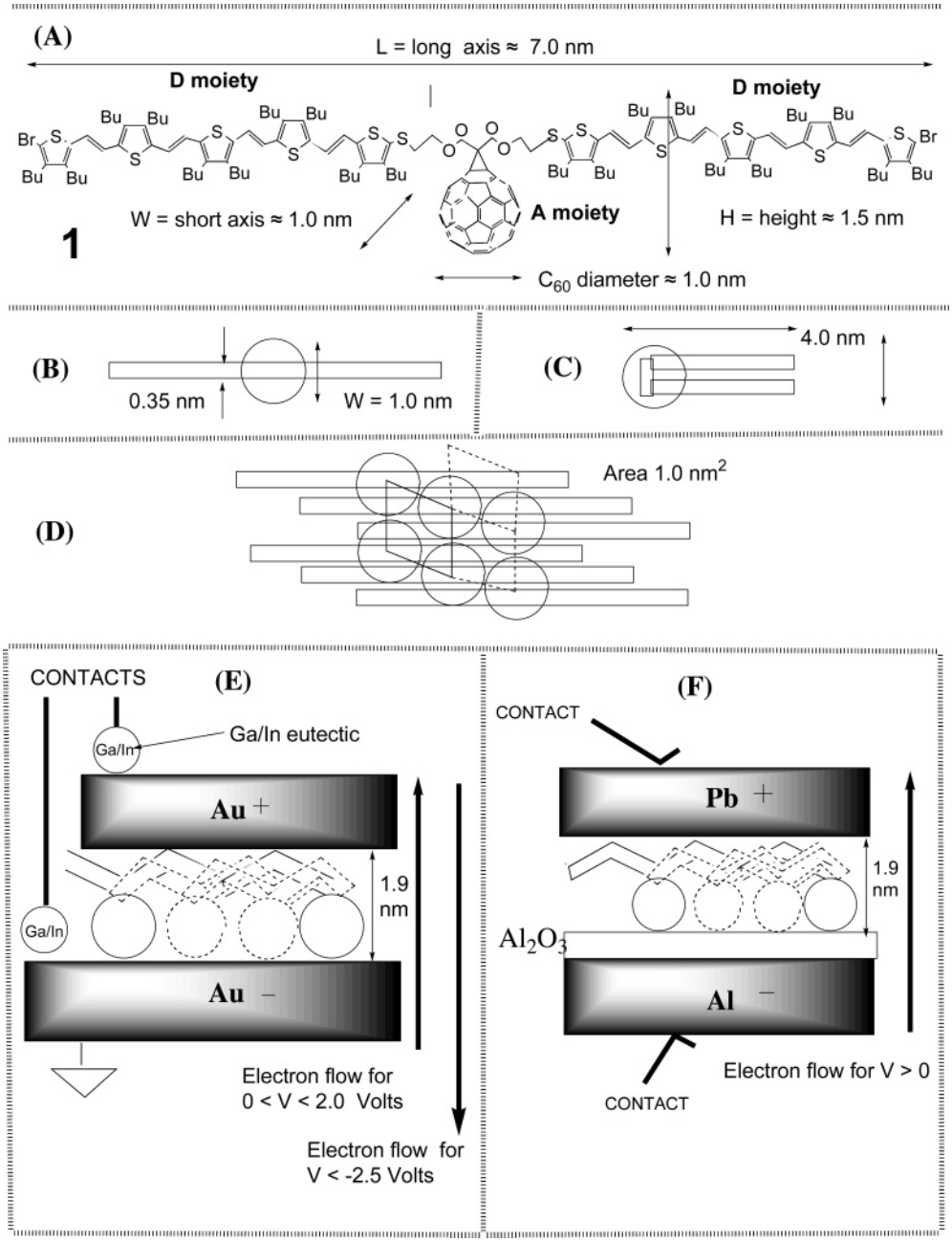

Figure 1. (A) Molecular structure of fullerene-*bis*[ethylthio-tetrakis(3,4-dibutyl-2-thiophene-5-ethenyl)-5-bromo-3,4-dibutyl-2-thiophene] malonate, molecule **1** in fully extended conformation; length L = long axis ≈ 7.0 nm, height $H \approx 1.5$ nm, width W = short axis ≈ 1.0 nm. The two electron donor regions (thienylenevinylenes) are marked "D moiety", and the electron acceptor region (fullerene) is marked "A moiety". (B) Plane projection of the extended conformation of **1**, viewed from the fullerene side, showing the 1.0 nm thickness of the fullerene moiety and the minimum van der Waals thickness (0.35 nm) of the donor end. (C) Plane projection of a hypothetical maximally folded conformation, with thiophenes folded into a "U": height $H \approx 4.0$ nm, length $L \approx 1.0$ nm, width $W \approx 1.0$ nm. (D) Closest packing of extended conformation B, with donor moieties interlocking and placed above fullerene regions of adjacent molecules: estimated cross-sectional area ≈ 1.0 nm^2. **(**E**)** Side view of "Au|LS monolayer of **1**|Au" junction; the polarity shown on the electrodes is for $V > 0$. The left arrow indicates the direction of electron flow at $V > 0$ for $|V| \leq 2$ V, while the right arrow shows the direction of favored electron flow for $V < -2.5$ V. (F) Side view of "Pd|LS monolayer of **1**|Al" junction; the polarity of the electrodes is for $V > 0$. The arrow indicates the direction of electron flow at $V > 0$.

IETS spectra were acquired at 4.2 K by second harmonic detection in an immersion Dewar (BOC Edwards 60 L). The home-built IETS spectrometer consisted of a dc voltage source, a lock-in amplifier (LIA), a digital multimeter, a custom-made adder circuit, an ac source, and a PC microcomputer (Windows 98) controlled by a program using the Labview (National Instruments, Austin, TX, version 4.1) equipment interface and data acquisition system (see Supporting Information, Figure C). External sources of noise were minimized as well as possible. The dc bias scan range was limited to below ±1 V. Above this bias, the noise matched or exceeded any possible signal. Signals were obtained using a source modulation frequency of $\omega/2\pi \approx 150-200$ Hz and second harmonic detection of the (d^2I/dV^2) signal at 2ω. The spectrometer performance was verified with benzoic acid, whose measured spectra were in excellent agreement with the literature results (see Supporting Information, Figures D and E). The IETS vibrational peaks have an overall line width[31] (full width at half-maximum) fwhm $= [(\mathrm{NLW})^2 + (5.4k_BT)^2 + (1.7V_{acmod})^2]^{1/2} = 6.882$ mV $= 55.5$ cm^{-1} for a natural vibration line-width NLW = 1 mV, $T = 4.2$ K, $k_B =$

(31) Wang, W.; Lee, T.; Reed, M. A. *Rep. Prog. Phys.* **2005**, *68*, 523−544.

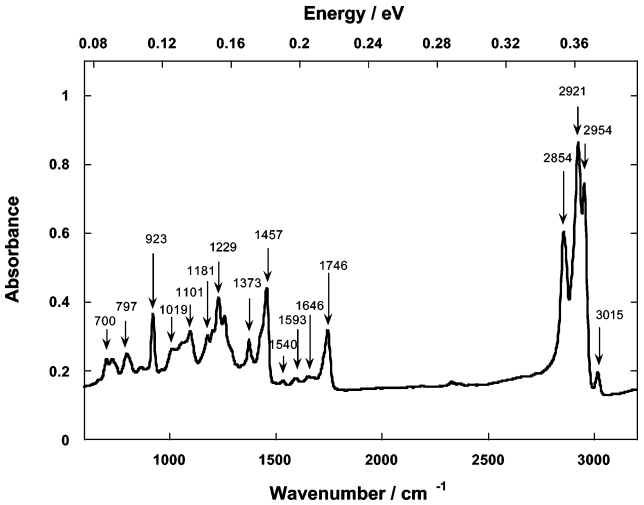

Figure 2. FTIR spectrum of bulk **1** in a KBr pellet.

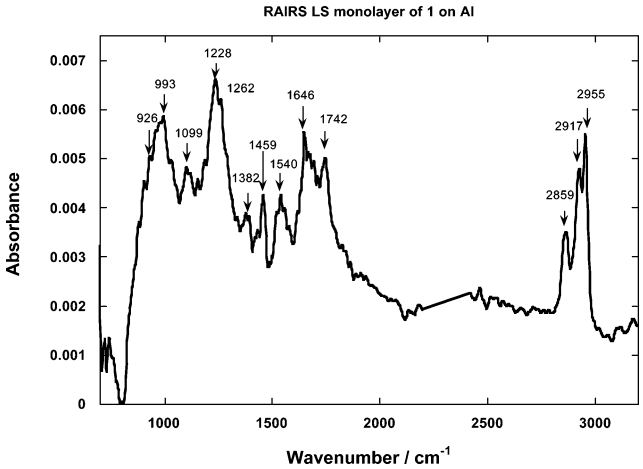

Figure 3. RAIRS spectrum of an LS monolayer of **1** deposited on Al.

Boltzmann constant, and an applied ac modulation voltage $V_{acmod} = 4$ mV. The dependence of fwhm on V_{acmod} was verified for the "Al|benzoic acid|Pb" junctions.[31] The energy conversion factor is 1 meV $\approx$ 8.065 cm^{-1}.

Results

Optical Spectroscopy of 1. The absorption spectrum of a solution of **1** in benzene shows a maximum at 529 nm, while the fluorescence emission spectral maximum occurs at 622 nm (Supporting Information, Figure F). The vertical band gap for molecule **1** determined from the UV−vis spectrum absorption edge is ~2.0 eV.

The IETS spectrum discussed below requires that optical absorbance be measured also in the near-infrared (NIR) region. No optically allowed electronic transition was observed in the region between 650 and 3400 nm (Supporting Information, Figure G). The most intense IR absorption bands are due to the C−H asymmetric stretch at 2927 cm^{-1}.

The bulk FTIR spectrum of **1** in KBr is presented in Figure 2. The absorption band at 923 cm^{-1} corresponds to the vinylene CH_2 in-phase, out-of-plane wag.[32,33] The very weak peaks at 1540, 1593, and 1646 cm^{-1} may be vinylene C═C stretch modes. The $-CH_3$ umbrella bending mode at 1373 cm^{-1} and the n-butyl group $-CH_2$ scissors mode[33] at 1457 cm^{-1} are intense. The vinyl CH_2 stretch appears at 3015 cm^{-1}, the asymmetric sp^3 CH_2 stretch is at 2954 cm^{-1}, the asymmetric sp^2 CH_2 stretch is at 2921 cm^{-1}, and the sp^2 symmetric CH_2 stretch appears at 2854 cm^{-1}. The ester −C═O bond is a prominent peak at 1746 cm^{-1}. The ester C−O−C stretches are at 1019 and 1101 cm^{-1}. One T_d C_{60} vibration[34] is clearly seen at 1181 cm^{-1}. The other T_d C_{60} vibration (expected[34] between 1429 and 1432 cm^{-1}) and the thiophene ring C═C stretch (expected[33] at 1436 cm^{-1}) are here in an unresolved shoulder of the very intense n-butyl $-CH_2$ scissor peak at 1457 cm^{-1}.

Monolayer Deposition. The PL isotherm (Supporting Information, Figure H) of molecule **1** shows three phases with the monolayer compression at the air−water interface. The first phase corresponds to the case where the molecules are dilute, gaseous, up to an area of ~250 Å^2. Further compression brings the molecules closer into a quasi-2-dimensional liquid phase, which persists up to ~200 Å^2. The monolayer is fully compressed into a 2D-quasi solid phase above ~10 mN m^{-1}. The area per molecule at zero film pressure is 270 Å^2; at transfer, it is 113 Å^2. The solid-like PL monolayer was transferred onto solid substrates via the LS horizontal technique at a pressure of ~20 mN m^{-2}. The LS transfer ratios were high (110−120%), probably because the molecules also deposited on the rougher substrate edges. LS monolayers of **1** were deposited onto Au, Al, and Si substrates.

Attempts to transfer the monolayer from the water by the LB or vertical transfer method gave only low transfer ratios, below 70%.

Molecular Orientation and Thickness Measurements. Molecular orientation studies carried out with XPS-angle resolved and grazing-angle reflection−absorption infrared spectroscopy (RAIRS). The RAIRS spectrum of the LS monolayers deposited on the Al surface (Figure 3) shows important changes in absorbance, when compared with Figure 2, due to surface dipole selection rules. The aliphatic C−H vibrations at 2965 cm^{-1} can be taken as intensity reference bands, because they are prone to conformational freedom on the surface. The vinyl ═C−H stretches present in the bulk at 3015 cm^{-1} (Figure 2) are absent on the Al surface (Figure 3): these bonds are parallel to the surface. The −C═C− and the C═O stretches of the ester at 1646 and 1742 cm^{-1} are greatly enhanced, compared to bulk, indicating that their bond dipoles are oriented perpendicular to the metal surface. The readily identifiable intensities of the various C═C modes of the thienylene rings and the vinyl group in the 1457−1646 cm^{-1} region are also enhanced; the tetrakis-(thienylvinylidene) moiety appears to have its long axis oriented parallel with the metal surface, as depicted in Figure 1A. The exact conformation of the two tetrakis(thienylvinylene) chains is difficult to determine, because conformational movements around the C═C bond of the vinylidene and isomerization of C−C bond between vinylidene and thienylene ring can cause disorder. Also, the XPS angle-resolved data (see Supporting Information, Figures I and J) show that the outer surface of the LS monolayer on Al is both C-rich and S-rich, indicating that the S atoms are preferentially on the outmost surface of the LS monolayer. The O atoms lie somewhat below the surface (negative slope of plot of the natural logarithm of the intensity versus

(32) Furukawa, Y.; Sakamoto, A.; Tasumi, M. *J. Phys. Chem.* **1989**, *93*, 5354−5356.
(33) Bolognesi, A.; Catellani, M.; Musco, A.; Pontellini, R. *Synth. Met.* **1993**, *55*−*57*, 1255−1259.
(34) Chase, B.; Herron, N.; Holler, E. *J. Phys. Chem.* **1992**, *96*, 4262−4266.

Table 1. Measured Monolayer Thickness (by XPS and Ellipsometry) and the Contact Angle of a Drop of Water over the Monolayer

substrate	thickness XPS (nm)	thickness ellipsometry (nm)	water contact angle (deg)
Al	2.3 ± 0.8		93.8
Si		1.89 ± 0.1	92.5
Au		1.83 ± 0.1	92.5

the cosecant of the angle Θ). On the basis of the slope, ~0.17, and the inelastic mean free path within an organic monolayer, which is typically between 22 and 27 Å for an electron kinetic energy of 720 eV, one can estimate that O atoms are approximately 0.6 nm below the outermost LS monolayer surface.

On the basis of this spectroscopic evidence, the molecular orientation is such that the C_{60} moieties are closest to the surface of the metal surface, while the carbonyl groups of the malonate ester are perpendicular to the surface, and the tetrakis(thienylene vinylidene)s are placed so that their long axes stretch sideways from the fullerene, possibly parallel to, or at small angles to, the metal surface. The measured organic monolayer thickness data obtained by XPS depth profiling and by spectroscopic ellipsometry are presented in Table 1, together with the contact angle of a water droplet atop the monolayer. The organic monolayer was modeled as two Cauchy layers with refractive indices 2 and 1.5.

Monolayer Structure and Orientation within the MOM Junctions. The structure of the PL and LS monolayer can be deduced by combining the pressure−area isotherm (Supporting Information, Figure H**)** with the XPS and FTIR results. The molecular structure, shown in Figure 1A, has been optimized by AM1 calculations (HyperChem), which yield a linear donor structure atop the C_{60} acceptor, with approximate dimensions $L \approx 7.0$ nm, $W \approx 1.0$ nm (corresponding to the diameter of C_{60} = 1.0 nm),[35] and $H \approx 1.5$ nm. The van der Waals thickness of the oligothienylenevinylenes, if planar, is 0.35 nm (Figure 1B). The C_{60} moiety is the more hydrophobic group. The LS monolayer thickness is 1.9 nm (Table 1), or slightly less than two C_{60} diameters; this means that the two donor arms cannot fold and extend vertically above the C_{60} acceptor (Figure 1C), because this would yield a film thickness of 4.0 nm. The XPS data also indicate that the O and S atoms are at 0.6 and 0 nm, respectively, from the outermost monolayer surface. The area per molecule in the LS monolayer at the transfer pressure estimated from the Langmuir isotherm (Figure H) is $A_t = 1.13$ nm^2, which is 11% larger than the area of one C_{60} molecule. If molecules **1** are accosted side by side, with no overlap, the area per molecule is estimated to be ≈2.5 nm^2, i.e., much larger than the area at the transfer pressure. However, if the donor arms lie somewhat above the C_{60} eicosahedra of neighboring molecules, and exhibit the intermolecular $\pi-\pi$ cofacial packing that is observed in some 3,4-n-butyl substituted oligothiophene crystals,[36,37] then the interlocked structure of Figure 1D yields the desired area ≈1 nm^2, and a minimum film thickness of 1.5 nm. With some bending of the thienylenevinylenes, this thickness can easily become 1.9 nm. This interlocked structure explains all the measured data for the PL and LS monolayers, and explains why LB transfer is impossible: the film is too rigid, and can be transferred only by quasihorizontal LS transfer.

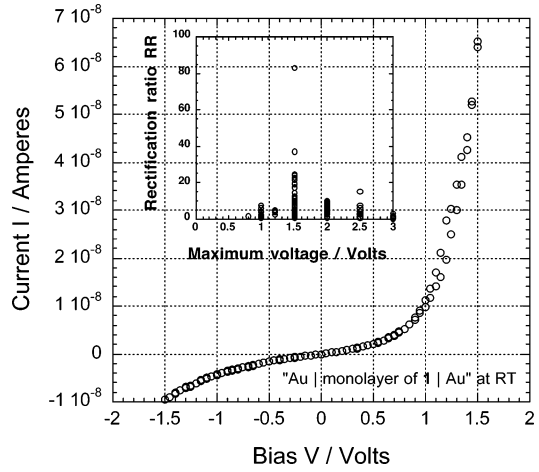

Figure 4. $I-V$ curve for "Au|monolayer of **1**|Au" junction (no. 18) at room temperature and for a smaller bias range ($|V| \leq 1.5$ V). The turn-on bias for rectification is $V \approx 0.8$ V. Inset: rectification ratios RR = $I(V_{max})/I(-V_{max})$ for all $I-V$ measurements at room temperature for $V_{max} \leq 3$ V.

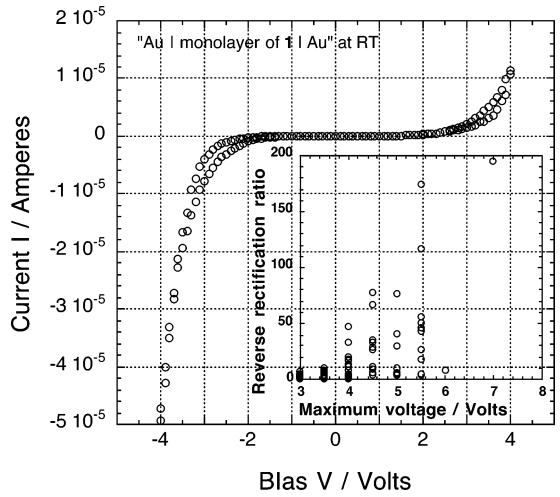

Figure 5. $I-V$ curve for "Au|monolayer of **1**|Au" junction (no. 9H2) at room temperature and larger bias range. The turn-on bias for rectification is $V \approx -2.5$ V. Inset: Reverse rectification ratios RRR = $I(-V_{max})/I(V_{max})$ for $I-V$ measurements at room temperature for $V_{max} \geq 3$ V.

Figure 1E,F shows how an LS monolayer of **1** can be arranged between Au electrodes (Figure 1E) and between Pb and Al electrodes (with the concomitant oxide coverings) (Figure 1F), and indicates, as explained below, the direction of electron flow through the monolayer at forward bias ($0 < V < 2.0$ V) or at large reverse bias ($V < -2.5$ V).

***I−V* Measurements.** The LS monolayers of **1** on Au were used for electrical $I-V$ measurements at room temperature in "Au|LS monolayer of **1**|Au" junctions, while the "Al|LS monolayer of **1**|Pb" junctions were used for $I-V$ measurements at 4.2 K.

The LS monolayers of **1** sandwiched between two Au electrodes exhibit current rectification at room temperature (Figures 4 and 5). But there are two regimes. (i) For $V_{max} \leq 2$ V, the higher currents are at positive bias ($V > 0$) (Figure 4) with rectification ratios (RR ≡ $-I(V_{max})/I(-V_{max})$ between 3 and 5 (forward bias corresponds to the top electrode (Au) being biased positively, and the bottom Au electrode biased negatively). (ii) For $V_{max} \geq 2$ V, the higher currents are at negative

(35) Yang, S. H.; Pettiette, C. L.; Conceiçao, J.; Chesnovsky, O.; Smalley, R. E. *Chem. Phys. Lett.* **1987**, *139*, 233−238.
(36) Huang, W.; Masuda, G.; Maeda, S.; Tanaka, H.; Ogawa, T. *Chem. Eur. J.* **2006**, *12*, 607−619.
(37) Pappenfus, T.; Raff, J. D.; Hukkanen, E. J.; Burney, J. R.; Casado, J.; Drew, S. M.; Miller, L. L.; Mann, K. R. *J. Org. Chem.* **2002**, *67*, 6015−6024.

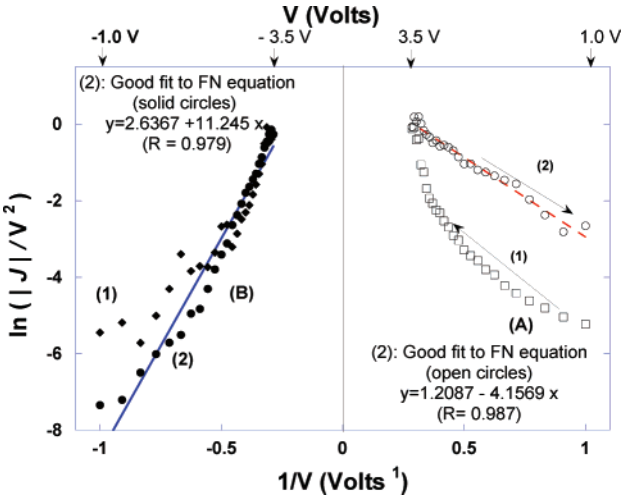

Figure 6. **(A)** Fowler−Nordheim plot of part of the $I-V$ data for "Au|monolayer of **1**|Au" junction (no. 1H3.1) at room temperature: poor least-squares linear fit for data measured for increasing positive bias, from $V = 1$ V to $V = 3.5$ V; very good least-squares linear fit (R= 98.7%) for data measured thereafter at decreasing bias, from $V = 3.5$ V to $V = 1.0$ V. **(**B**)** Same plot, but for negative bias: good fit for data from $V = -3.5$ V to $V = -1.0$ V.

bias ($V < 0$). At bias ranges above ±2.5 V, the rectification changes sign, with higher currents for $V < -2.5$ V (Figure 5), as observed recently for a chemically very similar fullerene derivative:[9] the currents are comparatively higher, and the reverse rectification ratios are larger in this higher-bias regime.

A summary of all $I-V$ data with Au electrodes is given in Table A of the Supporting Information, which also has two more $I-V$ curves (Supporting Information, Figures K and L).

When the applied biases exceed the tunneling barrier height $E_{LUMO} - E_{F(Au)}$, then cold-electron emission can also occur from the rougher electrode (e.g., the top electrode). This emission has been described by the Fowler−Nordheim (FN)[24,31,38,39] equation $JV^{-2} = (144e^3/529\pi hBd^2)\exp(-23^{1/2}\pi m^{1/2}B^{3/2}s/6ehV)$, where J is the current density, V is the voltage (V), B is the tunneling barrier relative to the electrode Fermi level $E_{F(Au)}$, e is the electronic charge, m is the mass of the electron, h is Planck's constant, and d is the gap between electrodes (here d = 19 Å). As seen in Figure 6A, the FN equation fits rather well for relatively high potentials (positive and negative), upon return from the extrema (V_{max} or $-V_{max}$) toward lower voltages, but fits poorly when these extrema are first approached from zero bias. In Figure 6 the absolute value of the current density J is 1.0 A m^{-2} at $V = |3.5$ V$|$. The slopes of the least-squares straight line fits are significantly different for positive and negative bias: the currents are larger when the electrons travel 1.9 nm from the "cold-gold" top Au electrode, which has the rougher surface, to the smoother bottom Au electrode. Is this asymmetry in surface roughness enough to explain the asymmetry in currents at room temperature seen in Figure 5?

For comparisons with the IETS reported below, the $I-V$ curve was also measured for an "Al|LS monolayer of **1**|Pb" junction at 4.2 K (Figure 7). The $I-V$ curve is asymmetric, RR ∼ 5. This correlation between the rectification ratio and the absolute intensity ratio of the broad bands, at negative and positive biases, holds well for most of the MOM junctions analyzed. However,

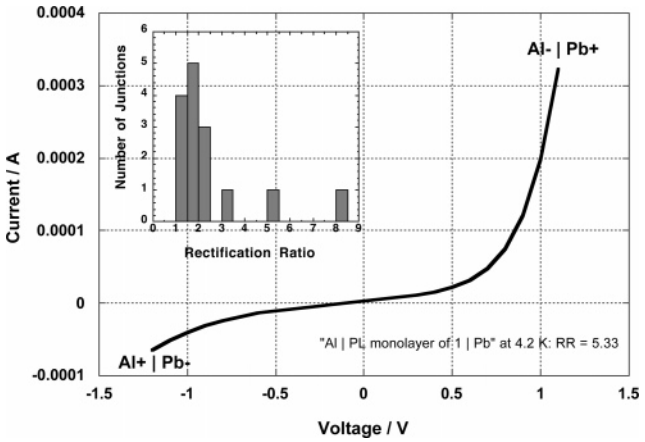

Figure 7. $I-V$ curve of an "Al|LS monolayer of **1**|Pb" junction (no. 13) at 4.2 K (RR = 5.33). The turn-on voltage is about 0.6 V. This is the same junction as measured by IETS in Figure 9. Inset: Histogram of the rectification ratios of "Al|LS monolayer of **1**|Pb" junctions at 4.2 K

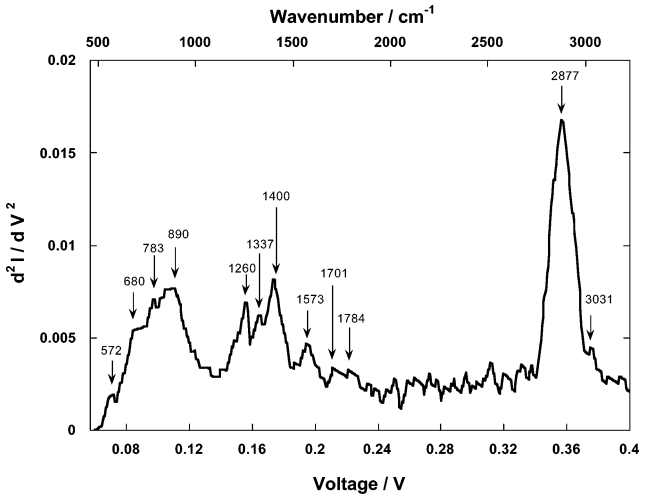

Figure 8. The IETS vibrational region spectrum (d^2I/d^2V) of an "Al|LS monolayer of **1**|Pb" junction (no. 9). The spectrum was acquired at 4.2 K (ac excitation signal V_{acmod} = 6.4 mV, frequency ν = 170 Hz).

a few junctions did not show broad bands, although they exhibited small current asymmetries in the $I-V$ curves (RR < 2). For applied voltages below 1.0 V, the rectification ratios are naturally slightly smaller, between 1 and 3. A histogram (inset to Figure 7) of the $I-V$ curves and the distribution of the number of junctions analyzed with the RR of the LS monolayers of **1** sandwiched between Al and Pb electrodes indicate that the RRs converge to RR ≈ 2.

A possible FN regime for the "Al|LS monolayer of **1**|Pb" junction at 4.2 K cannot be discussed here, since the required high-voltage regimes were not accessible in our IETS measurements.

IETS Measurements. The IETS spectrum for an LS monolayer of **1** sandwiched between Al and superconducting Pb electrodes is given in Figure 8 for the energy range 0.06−0.40 eV (500−3200 cm^{-1}). All the molecular vibrations, either Raman-active or FTIR-active, appear together in the spectrum, since electric dipole selection rules do not apply for IETS. The energy resolution for the IETS spectra, calculated as ∼55 cm^{-1}, is inferior to that of FTIR or Raman spectroscopy (less than ∼8 cm^{-1}). IETS peaks are seen at 572, 680, 783, 890, 1260, 1337, 1400, 1573, 1701, 1784, 2877, and 3031 cm^{-1}. These

(38) Fowler, R. H.; Nordheim, L. *Proc. R. Soc. London* **1928**, *119*, 173.
(39) Simmons, J. G. *J. Appl. Phys.* **1963**, *34*, 2581−2590.

Table 2. Comparison of IETS, RAIRS, and Bulk FTIR Spectra of **1** with Raman Spectra of Poly(thienylenevinylene) (PTV)[32,40] and of C_{60},[34] FTIR Spectrum of Poly(3,4-dibutylthienyl-enevinylene) (PbuTV),[33] IETS of Stearic Acid, $C_{17}H_{35}COOH$ ($C_{17}Ac$),[41] and of n-Octanethiol, $C_8H_{17}SH$ (C_8SH),[42] and Interpretation of the IETS Spectrum of **1**

FTIR bulk **1**	RAIRS mono **1**	IETS mono **1**	Raman PTV[32]	Raman PTV[40]	FTIR PbuTV[33]	Raman C_{60}[34]	IETS $C_{17}Ac$.[41]	IETS C_8SH[42]	interpretation of IETS of mono **1**
		572		557		569			T_d of C_{60}
700		680w	649	654					R def
797		783w		741		772	733		R def
							778		
				832					
				834			843	863	
							882		
923	926w	890	929		919		902		V CH bend
							950		
1019w	993						996		
				1040			1032		
			1045	1045			1074	1073	
1101w	1099w					1100	1113		
1181w				1169			1140		
1229	1228	1260	1285	1212		1250			V in CH bend
				1239					
				1275				1274	
				1287					
				1288			1312		
1373m	1373m	1337w		1350					
				1354			1367		
1457	1459	1400	1409	1410	1436	1425	1448		R CHstr/C_{60}
				1412					
				1488	1464	1468	1468		
						1481		1500	
1540w	1540	1573	1584	1586		1574			V C═Cstr/C_{60}?
1593w							1601		
1646w	1646								
1746	1742	1701							ester C−O str
		1784							ester C═O str
2854	2859	2877						2879	asym CH_2 str
2921				2917					
2954	2955	3013							as V CH str

peaks can be identified by comparison with literature[32−34,40−42] (Table 2) as follows: a weak vinylene C−H stretch at 3031 cm^{-1}, an intense symmetric CH_3 stretch at 2877 cm^{-1}; an ester C═O stretch at 1784 cm^{-1}; an ester C−O stretch at 1701 cm^{-1}, shifted to somewhat higher energies than in FTIR; a combination of a T_d vibration of C_{60} with a vinyl C═C stretch at 1573 cm^{-1}; a thiophene ring C−H stretch at 1400 cm^{-1}; a vinyl C−H bend at 1260 cm^{-1}; a nonplanar vinyl C−H bend at 890 cm^{-1}; thiophene ring deformations at 783 and 680 cm^{-1}; and a T_d vibration of the C_{60} moiety at 572 cm^{-1}.

The Broad Bands. At larger biases (Figure 9), antisymmetric broad bands appear at $\sim +0.66$ V and also at ~ -0.60 V. The ratio between the intensity of these bands, at positive and negative bias, measured from zero (Figure 9), is ~1.7. This broad band is more intense at forward bias, i.e., in same direction as the preferred electron flow observed in the $I-V$ curves (Figure 7). The asymmetry in the broad bands is preserved in a normalized tunneling intensity (NTI) spectrum representation (inset of Figure 9); the sloping background is removed by plotting $(d^2I/dV^2)/(dI/dV)$, instead of (d^2I/dV^2), versus V.[29]

The vibronic features of the IETS spectra acquired for the positive and negative biases are antisymmetric. The C−H bond vibration peaks appear to have different intensities at opposite polarities: The intensities are larger for Al electrode biased positively. This could be due to the molecular orientation: the CH groups are closer to the Pb electrode and couple better with the Pb electrodes. The organic monolayer is separated from the bare Al electrode by Al_2O_3. Such asymmetry has been discussed theoretically.[43]

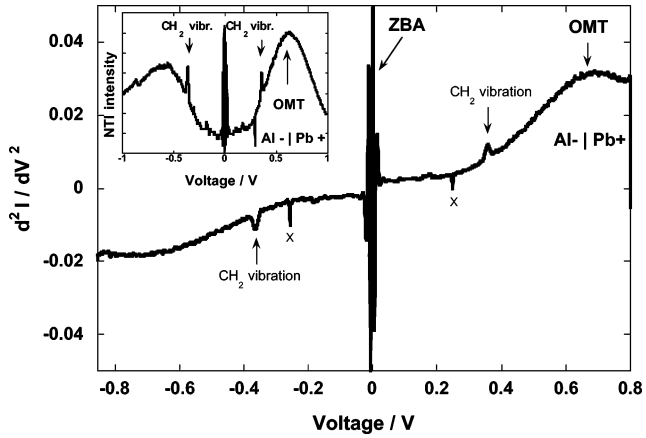

Figure 9. Wider-range IETS scan of an "Al|LS monolayer of **1**|Pb" junction (no. 13), showing the (a) ZBA, (b) dominant CH_2 peaks, (c) electronic artifacts marked "X", and (d) broad OMT feature at ~0.65 V: RR(V = 0.65 V) = 1.8. This is the same junction as measured in Figure 7. The inset shows the normalized tunneling intensity (NTI) spectrum, showing that the asymmetries of the OMT bands are preserved after background removal.

(40) Mevellec, J. V.; Buisson, J. P.; Lefrant, S.; Eckhardt, H. *Synth. Met.* **1991**, *41−43*, 283−286.
(41) Brousseau, J.-L.; Vidon, S.; Leblanc, R. M. *J. Chem. Phys.* **1998**, *108*, 7391−7396.
(42) Wang, W.; Lee, T.; Kretschmar, I.; Reed, M. A. *Nano Lett.* **2004**, *4*, 643−648.
(43) Galperin, M.; Nitzan, A.; Ratner, M. A.; Stewart, D. R. *J. Phys. Chem. B* **2005**, *109*, 8519−8522.

At near-zero bias, intense and narrow bands appear: These have been traditionally called zero-bias anomalies (ZBA), and are presumably due to Pb phonons within the superconducting Pb electrode.[44]

On a different junction (Supporting Information, Figure M), RR = (signal at 0.65 V/signal at −0.65 V) is smaller than in Figure 9, and the ZBA signals are also weaker. Two other junctions have essentially identical features to Figure 9 (Supporting Information, Figures N and O).

In Figure 9, the OMT bands appear at the same "turn-on" voltage obtained from the interpolation of the $I-V$ curve with the voltage, Figure 4, i.e., at ca. 0.7 V at forward bias.

A series of oscillations in the inelastic tunneling spectra of "Al|Al_2O_3|Pb" junctions have been studied in detail, and were dubbed the "quantum size effect" (QSE).[45−47] The QSE oscillations were observed between 0.4 and 1.4 V, with a center at 0.85 V,[45] and are due to particle-in-a-box standing-wave states in the superconducting Pb electrode;[45] they need a well-formed aluminum oxide barrier, depend explicitly on the Pb electrode thickness, and are absent for $V < 0$.[46] A plot of the QSE oscillation periods is linear with the reciprocal of the Pb layer thickness.[45] For the Pb layer thickness of 600 nm used here, the period of these oscillations should be 0.037 V.[45] Since no such period is seen in Figure 9, or in Supporting Information Figures M, N, or O, and since a weaker broad band is visible for $V < 0$, therefore[46] the broad bands of the present study are not due to QSE oscillations.

The broad bands observed in this study could be ascribed to either (1) inelastic scattering, due to an electronic transition in the molecule, or (2) elastic scattering, i.e., as a consequence of the enhanced electron flow due to resonance.

In an unrelated organometallic system, low-energy (∼5000 cm^{-1}) dipole-allowed and spin-allowed optical electronic transitions were observed, both optically and in IETS. The latter, elastic peak was given the name "orbital-mediated tunneling" (OMT).[29] Here, spin-allowed and dipole-allowed inelastic processes involving an electronic transition are ruled out, because around 5200 cm^{-1} (0.65 eV) the NIR spectrum of **1** (Supporting Information, Figure G) shows no electronic transition; also, the chemical structure of **1** makes an optical absorption unlikely at such low energies. The addition to, or subtraction from, a molecular orbital could be inelastic, but would be observable in electrochemical (not optical) experiments.

The second, elastic hypothesis may appear unusual, since the name of the method is IETS. However, the electron tunneling measurements with a lock-in amplifier measure the increase in the total current, rather than an abrupt change in the $I-V$ slope ("kink") at a particular voltage, caused by a scattering process and opening of a second tunneling channel.[48] A resonant tunneling process, in which an empty molecular orbital is brought into resonance, at a particular voltage, with the Fermi energy of a metal would also produce a change in the $I-V$ slope, and thus will be observed in the second harmonic measurement of d^2I/dV^2, as in IETS. Therefore, for the particular molecular junction investigated here the broad bands observed can be understood in terms of current flow enhancement, because at some bias the Fermi level of the electrode and a relevant molecular orbital are brought to the same energy. For molecule **1**, the probed relevant molecular orbital, i.e., the LUMO, mediates the electron tunneling at both positive and negative bias. At positive bias the potential, at which this broad band appears (0.6 V), is roughly twice the $E_{F(Al)}$ − LUMO gap; at negative bias the band appears at −0.66 V, or twice the $E_{F(Pb)}$ − LUMO gap. On the basis of the above considerations, the LUMO energy is placed at roughly −3.9 eV with respect to vacuum. In the above calculations, the electrode work-functions were 4.17 eV for Al and 4.2 eV for Pb, as determined from photoelectron measurements.[49] The difference in IETS intensities at +0.60 and −0.66 V, and the difference in currents in the $I-V$ curves at these two potentials, can be explained by the greater proximity of the LUMO to the Al electrode than to the Pb electrode (neglecting the defective Al oxide, for IETS) or to the bottom Au electrode (for the $I-V$ curves), which makes for a more efficient coupling at forward bias ($V > 0$) than at reverse bias. The width of the two OMT bands is due to either (a) the polycrystallinity of the metal electrodes, whose Pb and Al crystallites have random orientation, or (b) the vibronic envelope that widens any electronic transition in the molecule. For explanation (a), the broadening would be due to a sample-average range of crystallite orientations with a concomitant range of work-functions. Indeed, the Al work-function values are 4.20 eV for the (100) face, 4.06 eV for the (110) face, and 4.26 eV for the (111) face, is ∼4.17 eV, while the value for polycrystalline Pb is 4.25 eV.[49] For explanation (b), Figure F suggests a 1 eV width for an allowed optical transition.

If the above interpretation of the broad band is correct, then one can probe with IETS the molecule's affinity level (electron affinity) and the creation of a molecular anion. OMT bands have been previously observed in IETS; the process of "molecular excitation to an affinity level" and determination of the "vertical attachment energies" were previously suggested by Hipps and Mazur.[25,50]

The LS monolayers of **1** are structured, and the molecules are oriented asymmetrically on the surface: Thus, the current asymmetry observed in IETS may be mostly due to the different tunneling efficiencies from the "Pb|LS monolayer of **1**" side versus the "Al|LS monolayer of **1**" side of the MOM junction.

Among all the MOM junctions of **1** studied so far, the ratio between the broad-band intensities, in the d^2I/dV^2 versus V spectrum, for the forward versus the reverse bias, is found to be closely related to the rectification ratio observed in the $I-V$ curves. The higher band at forward bias is always more intense. The forward bias occurs in the same directions for $I-V$ ($|V| \leq 2$ V, Au electrodes) and IETS (Pb and Al electrodes). The fullerene moieties are closest to the negative electrode, and the thienylene−vinylene moieties are closest to the positive electrode. Previous studies[51] of current asymmetries in Al−AlO_x−Pb junctions, with various randomly oriented organic

(44) Wolf, E. L. *Principles of Electron Tunneling Spectroscopy*; Oxford University Press: Oxford, U.K., 1985; p 393.
(45) Jaklevic, R. C.; Lambe, J.; Kirtley, J.; Hansma, P. K. *Phys. Rev. B* **1977**, *15*, 4103−4104.
(46) Jaklevic, R. C.; Lambe, J. *Phys. Rev. B* **1975**, *12*, 4146−4160.
(47) Kipps, K. W.; Susla, B. P.; Dunkle, E. *J. Phys. Chem.* **1986**, *90*, 3898−3900.
(48) Hansma, P. K. *Phys. Rep.* **1977**, *30*, 145−206.
(49) *CRC Handbook of Chemistry and Physics*, 82nd ed.; Lide, D. R., Ed.; CRC Press, Boca Raton, FL, 2001−2002; p 12−130.
(50) Hipps, K. W.; Mazur, U. *J. Phys. Chem.* **1994**, *98*, 5824−5829.
(51) Muldoon, M. F.; Dragoset, R. A.; Coleman, R. V. *Phys. Rev.* **1979**, *B20*, 416−429.
(52) Honciuc, A. Ph.D. Dissertation, University of Alabama, August 2006.

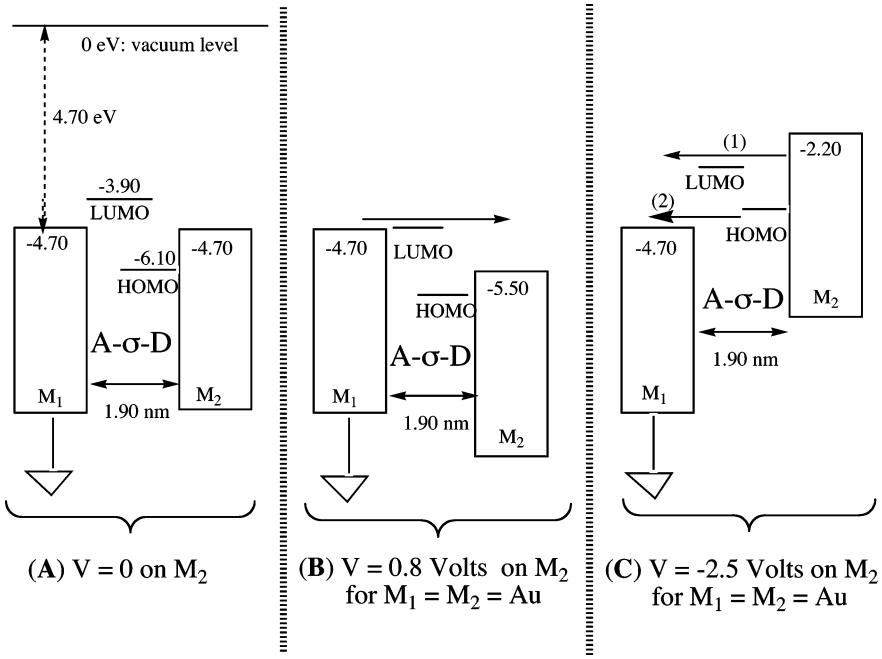

Figure 10. Proposed mechanisms for the two rectification modes of D-σ-A molecule **1**. The (bottom) metal electrode M_1 is grounded throughout. (A) At zero bias, the HOMO, mostly localized on the bis-tetrakis(thienylenevinylene)s, is closer to the bottom electrode, and the LUMO, mostly localized on the fullerene, is closer to the top electrode M_2. (B) At $V \geq 0.7$ V, the LUMO comes into resonance with the Fermi level of M_1, and resonant tunneling occurs through the orbital to the second electrode M_2. (C) At $V = -2.5$ V the LUMO comes in resonance with M_2, and the HOMO is in resonance with M_1: An electron moves from M_2 to LUMO (step 1), and an electron from the HOMO moves to M_1 (step 2, presumably in synchrony with step 1). This creates the excited state D^+-σ-A^-, which relaxes somehow to the ground state D^0-σ-A^0.

molecules interspersed between the alumina and Pb layers, show that the $I-V$ characteristic of a junction is strongly dependent on the adsorbate; the corresponding broad bands observed in IETS spectrum were attributed to "low-lying organic barrier heights", i.e., to $E_{F(metal)}$ − LUMO.[51]

Discussion

IETS measurements have yielded not only (1) the vibrational spectrum of an LS monolayer of **1**, but also (2) a broad and asymmetric signal due to the onset of molecular rectification and resonant tunneling between the metal electrodes and the molecule. This is the conclusive proof that the rectification we have been measuring for several years is indeed due to through-bond tunneling processes within the molecules.

The LS monolayer of **1** also shows two rectification regimes, one at relatively lower bias, and a different one at higher bias. (1) For $V_{max} \leq 2$ V the enhanced currents are for $V > 0$ [turn-on at 0.8 V for Au electrodes (Figure 4) and at 0.6 V for Pb and Al electrodes (Figure 7)], and (2) for $V_{max} \geq 3$ V and Au electrodes, the higher currents occur are for $V < 0$ [turn-on at −2.5 V] (Figure 5). The first rectification is most likely due to electrons accessing only the unoccupied orbitals, i.e., the LUMO, which should be localized on the fullerene moiety,[9] while the second rectification is probably due to two electron transfers, one from the metal electrodes to the LUMO on the fullerene acceptor moiety and the other from the HOMO on the thienylene−vinylene electron donor moiety to the Au electrode. This interpretation is schematically presented in Figure 10. The metal electrode M_1 is held at zero applied potential throughout. The work function of Au was taken as 4.70 eV (in the literature there is considerable variation of this value, from 4.70 to 5.40 eV, depending on the crystal face of Au and the method of measurement). In the following simplified discussion of electron transfer through an organic monolayer, it is assumed that the potential drop between the two metal surfaces occurs exclusively, but not linearly, across the monolayer.[9] It is further assumed that the oxide that formed on the Al electrode upon exposure to air is sufficiently thin and defective that an energy barrier across the oxide can be ignored.

We now have to place the HOMO and LUMO of the monolayer, relative to the metal work functions. The optical spectrum (Figure F) leads to a HOMO−LUMO gap of 2.2 eV. The onset of asymmetric conductivity suggests that the LUMO should be placed at −3.9 eV, even though the experimental gas-phase electron affinity of C_{60} is 2.8 eV.[35] Placing the HOMO 2.2 eV below the LUMO, at −6.1 eV, is also suggested by our $I-V$ data, even though the gas-phase ionization potential of the oligothienylenevinylenes is probably around 7.5 eV. To account for the molecular orientation, we have pinned the LUMO and the HOMO energies to the adjacent metallic electrodes M_1 and M_2, respectively. As the bias on electrode M_2 departs from zero, the HOMO and LUMO energies must change with the applied electric field within the 1.9 nm thick monolayer, as the Gibbs chemical potential (or Fermi level) shifts in response to the applied bias. This shift may not be linear with distance across the monolayer.[9]

The asymmetry in Figure 10B suggests that the current at moderate forward bias is larger than that at reverse bias, perhaps because the fullerene moiety is physically closer to the bottom Au electrode M_1 than to the top cold-gold evaporated Au electrode M_2. In contrast, in Figure 10C, at high reverse bias the favored electron transfer (M_2 to LUMO, HOMO to M_1) is to orbitals placed farther from the appropriate electrode.

While the work-functions for Pb and Al are very close to each other, there is a significant difference in the work-functions

of Au and Al (0.5−0.8 eV, depending on method and crystal facet): It is thus a bit surprising that the "turn-on" voltages are 0.8 V (Figure 4) for Au, but 0.60 V for Al + Pb (Figure 7). Previous experience[5] suggests that this difference (0.20 V) should be at least 0.5 V.

The good fit of the FN equation in Figure 6A gives, from its slope, a tunneling barrier height of ∼0.4 eV above the $E_{F(Au)}$, thus placing LUMO at −4.3 eV; this estimate places the LUMO 0.4 eV lower than the estimates from IETS (∼ −3.9 eV) or from the energy levels chosen in Figure 10 (∼ −3.9 eV). The HOMO may also be involved in the electron transport across the "Au|LS monolayer of **1**|Au" junction; this is also suggested by the strong hysteresis between the scans in opposite scan directions, and the bad fits of the FN equation for the return curves in Figure 6. Unlike resonant tunneling through a LUMO, which is an empty orbital readily available to an incoming electron, tunneling through an initially filled HOMO should involve two consecutive steps: first, "half-emptying" the HOMO, and next, "refilling" it.

For the positive bias case, +1 to +3.5 V in Figure 6A, where the HOMO is physically closer to the M_2 electrode than to the M_1 electrode, as shown in Figure 10C, the electron transfer from the LS monolayer of **1** to M_2 (emptying) may be faster than the transfer from M_1 to LS monolayer of **1** (filling). That is, the extraction of an electron from the HOMO may be somewhat adiabatic ("charge trapping"). This would contribute to the observed hysteresis in Figure 6A.

For the negative-bias regime, the FN fit, Figure 6B, gives a barrier height of ∼0.7 eV above the $E_{F(Au)}$, and a LUMO at ∼ 4.0 eV with respect to vacuum level, in better agreement with previous estimates. Here, the HOMO contribution to electron transport may be less, and less hysteresis is seen.

Barring further data analyses and experiments on other systems and, most importantly, upon overcoming experimental barriers in IETS, such as making low-resistance contacts to "Au|monolayer|Au" junctions that can remain ohmic under He temperatures, we consider the mechanism presented in Figure 10 to be a valid model of LS monolayer rectification.

Conclusion

The rectification by a single molecule in an LS monolayer has been confirmed by d^2I/dV^2 measurements at 4.2 K between Al and Pb electrodes as due to electrons from the metal electrode transferring resonantly to the available LUMO of the molecule. This orbital-mediated tunneling is asymmetric and opposite in sign with respect to junction polarities, and occurs at the same voltage as the onset of enhanced current flow in direct-current measurements. IETS vibrational spectra were also measured. At much higher potentials, the current asymmetry is reversed: At sufficiently high bias, both HOMO and LUMO can be accessed from the metal electrodes.

Acknowledgment. We are grateful to Mr. Gihan Kwon for assistance with XPS data collection, and to Professors Patrick LeClair (University of Alabama), Gregory J. Szulczewski (University of Alabama), Mark A. Reed (Yale University), and Kerry W. Hipps (Washington State University) for helpful discussions. The IETS equipment was acquired using residual funds of Grant NSF-DMR-00-95215. A.G. was supported by DOE-EPSCoR.

Supporting Information Available: Synthesis and characterization details, a schematic diagram of the IETS spectrometer,[52] IETS spectra of benzoic acid,[52] the UV−vis and fluorescence spectra of solutions of **1**, the near-IR spectrum of a film of **1**, the PL isotherm of **1**, the XPS intensities for a monolayer of **1** as functions of the takeoff angle, a table of all the $I-V$ measurements of monolayers of **1** between Au electrodes at room temperature, two $I-V$ curves of a monolayer of **1** between Au electrodes at room temperature, IETS spectra of **1** between Al and Pb electrodes at 4.2 K for a narrower-range scan (−0.6 to 0.6 V) and for wider-range scans (−0.7 to 0.7 V). This material is available free of charge via the Internet at http://pubs.acs.org.

JA068729G